Approximation of Internal Refractive Index Variation Improves Image Guided Diffuse Optical Tomography of Breast

Ravi Prasad K. Jagannath and Phaneendra K. Yalavarthy*

***Abstract*—Effective usage of image guidance by incorporating the refractive index (RI) variation in computational modeling of light propagation in tissue is investigated to assess its impact on optical-property estimation. With the aid of realistic patient breast three-dimensional models, the variation in RI for different regions of tissue under investigation is shown to influence the estimation of optical properties in image-guided diffuse optical tomography (IG-DOT) using numerical simulations. It is also shown that by assuming identical RI for all regions of tissue would lead to erroneous estimation of optical properties. The *a priori* knowledge of the RI for the segmented regions of tissue in IG-DOT, which is difficult to obtain for the *in vivo* cases, leads to more accurate estimates of optical properties. Even inclusion of approximated RI values, obtained from the literature, for the regions of tissue resulted in better estimates of optical properties, with values comparable to that of having the correct knowledge of RI for different regions of tissue.**

***Index Terms*—Biomedical optical imaging, image reconstruction, image registration, optical tomography.**

I. Introduction

DIFFUSE optical imaging uses near infrared (NIR) wavelengths between 600 and 1000 nm to obtain the optical images of tissue under investigation [1], [2]. Often the experimental data are collected on the boundary of the tissue and based on these limited measurements, the internal distribution of optical properties are reconstructed. When the data from multiple wavelengths are available, diffuse optical tomography (DOT) is capable of providing the functional images, in turn revealing the pathophysiological state of the tissue [2], [3]. Scattering dominance at NIR wavelengths makes the optical image reconstruction a nonlinear, ill-posed, and some times underdetermined problem [4]. Moreover, diffuse optical images lack good spatial resolution (spatial resolution $\sim$5 mm) [3]. Image guided DOT (IG-DOT) overcomes this problem, where the image guidance is generally through traditional medical imaging modalities, such as mammography, tomosynthesis, ultrasound, and MRI. Images obtained from traditional medical imaging modalities typically have good spatial resolution ($\sim$1 mm), but may not have the same capabilities as diffuse optical imaging in providing the functional information [2], [3], [5], [6]. These types of multimodal approaches (IG-DOT) have been reported in the literature and shown to be more effective, in terms of quality and quantitation of optical images, compared to traditional imaging approaches [2], [3], [5]–[8].

In IG-DOT, the image guidance is primarily in providing the structural information, either used in the regularization (known as "*soft priors*") or parameter reduction (known as "*hard priors*") of the optical image reconstruction procedure [7], [8]. Due to the computational complexity of the soft priors, the hard-priors approach is more sought after, especially in three-dimensional (3-D) diffuse optical imaging [8]. The hard priors approach reduces the parameter space (optical properties) into the number of regions segmented from the high-resolution imaging modality [7], [8]. In the example of breast, this can be adipose (fatty), fibro-glandular, and tumor [5]. As the number of optical parameters to be reconstructed is equal to the number of segmented regions, the image reconstruction problem tends to be a better determined problem, compared to the traditional reconstruction problem [8]. Earlier works presented in the literature have exploited this in providing high-resolution diffuse optical images in IG-DOT [6], [9]. It was also shown that in the case of breast imaging, combining MRI with DOT, the IG-DOT was capable of eliminating the false positives of MRI [6]. The effective image guidance in reconstructing diffuse optical images has been an active research area, and in this study, use of the region information to improve IG-DOT images by incorporating the refractive index (RI) variation is attempted.

In IG-DOT, the high-resolution images from traditional imaging modalities are used to obtain the finite-element meshes with segmented regions [9]. Identification/segmentation of these regions is an active area of research, as the uncertainties in the segmentation could influence the final outcome of the optical-image reconstruction procedure [2], [3], [7]. Typically, the diffusion equation (DE), which is valid for thick tissues, often solved on these meshes using finite-element method (FEM). Even though RI of each segmented region is known to be different [10], [11], a uniform RI is typically used in solving the DE [5], [7], [8], thus leading to inaccurate modeling of NIR light propagation in tissue [12], [13]. This uniform modeling of RI is primarily due to the fact that the RI for the segmented regions is often not known, especially in *in vivo*. Moreover, finding the RI distribution for the tissue under investigation should be posed as

Manuscript received March 31, 2010; revised May 23, 2010 and June 7, 2010; accepted June 11, 2010. Date of publication June 21, 2010; date of current version September 15, 2010. This work was supported in part by the Apple Research and Technology Support (ARTS) and Indian Institute of Science Mathematics Initiative (IMI). *Asterisk indicates corresponding author*.

R. P. K. Jagannath is with the Supercomputer Education and Research Centre, Indian Institute of Science, Bangalore, Karnataka 560012, India.

*P. K. Yalavarthy is with the Supercomputer Education and Research Centre, Indian Institute of Science, Bangalore, Karnataka 560012, India (e-mail: phani@serc.iisc.ernet.in).

Digital Object Identifier 10.1109/TBME.2010.2053368

a new reconstruction problem, which is not so straightforward in the case of unknown optical properties [14]. Earlier investigations in breast imaging, limited to two dimensions (2-D) (also not in the context of IG-DOT), have shown that the uniform modeling of RI will have minimal effect on the estimated optical properties [13]. This paper mainly aims to show that the approximation of internal RI values for the segmented regions (obtained from the literature) in IG-DOT will lead to improved estimates of optical properties. Note that the example shown in this paper pertained to MRI-guided DOT for 3-D breast cancer imaging. Results from cases where the exact RI is assumed to be known *a priori* are also presented for fair comparison along with the uniform RI cases. From the simulation studies, it will be shown that assuming uniform RI could lead to errors up to five times in terms of quantitation of optical properties in IG-DOT.

II. Methods

A. Diffusion-Based Forward Model

The light propagation in the breast tissue is modeled using the DE, which is an approximation to radiative transport equation (RTE) [4]. In the frequency domain, it can be written as follows:

$$-\nabla.D(r)\nabla\Phi(r,\omega) + \left(\mu_{\mathbf{a}}(r) + \frac{i\omega}{c}\right)\Phi(r,\omega) = Q_o(r,\omega) \tag{1}$$

where $\Phi(r,\omega)$ is the photon density at position r with the ω as the NIR light modulation frequency (=$2\pi f$, with $f = 100$ MHz). Speed of light in tissue is given by c (=C_v/n, with C_v representing the speed of light in the vacuum and n is the RI of the tissue) with isotropic source term represented by $Q_o(r,\omega)$. The optical absorption and diffusion coefficients are given by $\mu_a(r)$ and $D(r)$, respectively, with $D(r) = 1/[3(\mu_{\mathbf{a}}(r) + \mu'_{\mathbf{s}}(r))]$. Here, the $\mu'_{\mathbf{s}}(r)$ represents the reduced scattering coefficient, which is equivalent to $\mu_{\mathbf{s}}(1-g)$, with μ_s as the scattering coefficient and g as the anisotropy factor. The RI mismatch between the breast boundary and air is modeled by using a Type-III boundary (Robin-type) condition [15]. The DE is solved using the FEM [16] and the modeled data in the frequency domain are the natural logarithm of the amplitude and phase of the computed signal. This forward model is used repeatedly in an iterative procedure to estimate the optical properties of the tissue under investigation [4]. The RI modeling used in this paper is described in [12].

B. Estimation of Optical Properties Using Hard Priors

The estimation of optical properties in the hard-priors approach is performed using Levenberg–Marquardt (LM) minimization [8]. The objective function in this case is given by

$$\Omega = \|y - G(D,\mu_a)\|^2 \tag{2}$$

where G is the diffusion-based forward model described earlier and y is the experimental measured data. The aim of this approach is to match the modeled data ($G(D,\mu_a)$) with the experimental data (y) in the least-squares sense, by changing the optical properties (D,μ_a). This minimum is achieved when the first derivative of Ω (2) with respect to D and μ_a equal to zero. This leads to updated equation as follows [8]:

$$\left[\mathbf{J}^{\mathbf{T}}\mathbf{J} + \lambda\mathbf{I}\right](\triangle D, \triangle\mu_a) = \mathbf{J}^{\mathbf{T}}\left(y - G(D,\mu_a)\right) \tag{3}$$

where $\triangle D$ and $\triangle\mu_a$ are the updates in D and μ_a, respectively. $\mathbf{J}$ is the Jacobian matrix, which is the first derivative of forward model (G) with respect to optical properties (D,μ_a) and has the dimension of 2NM $\times$ 2NR in the case of IG-DOT, where NM represents the number of measurements and NR represents the number of regions. The multiplication of factor of 2 in the measurements is because of treatment of amplitude and phase of signal separately. The information of NR is obtained through the image guidance provided by the traditional imaging modality (here, it is MRI). In traditional DOT, NR is equal to number of FEM nodes present in the finite-element mesh. In the case of breast imaging, the NR is equal to three, representing fatty (adipose), fibro-glandular, and tumor regions [5]. λ in (3) represents the regularization parameter with a starting value of 1 (in this study) and reduced by $10^{0.25}$ in every iteration [8]. The iterative procedure is stopped when the Ω (2) did not improve by more than 0.001% in successive iterations.

The Jacobian ($\mathbf{J}$) in this paper is calculated using a perturbation approach, with $\mathbf{J} = (G(\mu+\delta\mu) - G(\mu))/\delta\mu$. Here, μ could be either D or μ_a and the $\delta\mu$ is 1% of the average value of μ. Even though the traditional method of calculation of $\mathbf{J}$ using adjoint method could also be employed, resulting in dimension of 2NM $\times$ 2NN (where NN represents number of FEM nodes), and subsequently, reducing it to 2NM $\times$ 2NR, as given in [7]. Note that the perturbation approach is more memory efficient as compared to the adjoint method, with later method requiring to store a large $\mathbf{J}$ (with NN = 10 000 or more in 3-D).

C. Simulation Studies Using Realistic 3-D Breast Models

To study the effect of RI variation on the estimation of optical properties using hard priors, we have considered six 3-D meshes in total. These were obtained from segmenting and meshing of MRI T1-weighted images acquired on Dartmouth MRI–NIR imaging system [17] on patients with breast cancer. The procedure of volumetric meshing and segmenting of these MRI images is given in [9]. These patient 3-D breast meshes are given an unique number (namely, 1915, 3007a, 1917, 501, 501c, and 1907), and each of the FEM node in these meshes are labeled to uniquely identify the three regions (adipose, fibro-glandular, and tumor) of the breast. Along with these regions, the source/detector locations are also identified to perform the image reconstruction procedure. In total, 16 fiber bundles (source/detector) were placed in contact with skin in the middle plane of the breast [shown as filled circles on the target μ_a distribution of Fig. 1 (second row, first column)] similar to Dartmouth MRI–NIR imaging system [17] and when one source is used as a source, rest acted as detectors, thus resulting in NM = 240 (16 $\times$ 15).

We have used the following properties (mimicking the typical breast [7], [11]) to generate numerical experimental data (with 1% noise added) to act as target meshes. The properties for adipose region: $\mu_a = 0.01$ mm^{-1}, $\mu'_s = 1.0$ mm^{-1}, and RI = 1.467; fibro-glandular region: $\mu_a = 0.015$ mm^{-1}, $\mu'_s =$

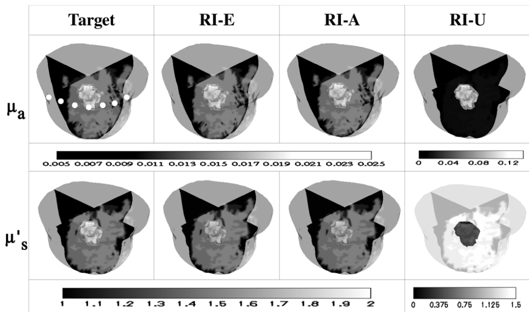

Fig. 1. Reconstructed distributions of (top) μ_a and (bottom) μ_s' using the three strategies discussed in Section II-C. (given on top of each column) along with the target distributions (first column) for 1915 mesh. The source/detector fibers are indicated by filled circles in the μ_a distribution of the target. The estimated optical properties for this 1915 mesh are also listed in Table I.

$1.5\ \mathrm{mm}^{-1}$, and RI $= 1.389$; and tumor: $\mu_a = 0.02\ \mathrm{mm}^{-1}$, $\mu_s' = 2.0\ \mathrm{mm}^{-1}$, and RI $= 1.390$. Three different strategies were employed in this study in regard to show the effect of RI on the optical-parameter estimation. They are given as follows along with the abbreviation for each of the strategy.

1) RI-U: The RI of each region is assumed to be uniform and equal to 1.467 (mimicking the adipose tissue values [11]).

2) RI-E: The RI of each region was same as used in the target mesh.

3) RI-A: The RI is approximated by taking the average values from the earlier reports [10]–[13], [18], for each region. These are for adipose region: RI $= 1.455$; fibro-glandular region: RI $= 1.4$; and tumor: RI $= 1.4$.

Note that in all three strategies, an uniform initial guess (same as the adipose) for the optical properties is used.

Further in case of RI-U strategy, to know the improvement in the optical property estimation with multilayer data, a numerical investigation that uses data from three fiber layers (fibers arranged similar to single plane) was also taken up. These three fiber layers (or rings) are 10 mm apart in the *Z*-direction (with one layer above and another below to the single layer), and when one fiber is used as a source, the fibers in the same fiber layer acted as detectors (three layers in-plane strategy in [19]), resulting in NM $= 720$ ($3 \times 16 \times 15$). As typical RI values of 1.4 and 1.33 are used in the literature under the uniform RI assumption [1], [5], an investigation with these values (along with 1.467) as test conditions is carried out to deduce a suitable RI that could be used in RI-U strategy.

The FEM meshes used in this paper had 12 000 nodes (up to 70 000) corresponding to 60 000 (up to 390 000) tetrahedral elements. The computations were carried out on a Linux workstation with dual quad-core Intel Xeon processor 2.33 GHz with 64 GB RAM. The typical computation time for each iteration was $\sim$3 (up to 8) min.

III. Results and Discussion

The reconstructed μ_a and μ_s' distribution using 1915 3-D breast mesh along with the target distribution (first column) are given in Fig. 1. The corresponding reconstruction strategies used to obtain the same are given on top of each column of Fig. 1. To analyze the results more carefully, the estimated optical properties for each region using three strategies mentioned in the Section II-C are compiled in Table I. It is evident from Table I and Fig. 1 that the estimated optical properties were erroneous when the RI was considered to be identical in all three regions of mesh, especially for cases of 1915, 501, and 501c. The error in estimating the optical properties μ_a & μ_s' in the tumor region of the cases mentioned are 505% and 98.5%, 55% and 39.5%, and 40% and 16.5%, respectively (see Table I and Fig. 1). Knowing the exact RI of each region gave better accurate results, but extracting the same information in *in vivo* cases is difficult and typically requires a new inverse problem to be formulated [14]. As it is evident from Fig. 1 and Table I that even an approximation of RI (RI-A), which was obtained by taking the average value of the RI using the literature [10], [13], [18], lead to better estimation of optical properties. In all six cases, the performance of RI-A strategy is at par with the RI-E (where RI is assumed to be known *a priori* for all regions). Moreover, in terms of computational complexity rather than using RI as an unknown, approximation of the same for different regions of tissue provides optimal solution.

TABLE I
Estimated Optical Properties (in mm^{-1}) of Each Region Using the Three Strategies Discussed in Section II-C for Six Meshes

Mesh	*Method*	*Adipose*		*Fibro-glandular*		*Tumor*	
		μ_a	μ_s'	μ_a	μ_s'	μ_a	μ_s'
Target	-	0.010	1.00	0.015	1.50	0.020	2.00
1915	**RI-U**	0.010	0.99	0.016	1.43	0.121	0.03
	RI-E	0.010	1.01	0.015	1.49	0.021	1.84
	RI-A	0.010	1.01	0.015	1.49	0.021	1.84
3007a	**RI-U**	0.011	0.99	0.015	1.54	0.019	2.07
	RI-E	0.010	1.00	0.016	1.43	0.019	2.10
	RI-A	0.010	1.01	0.016	1.46	0.019	2.11
1917	**RI-U**	0.010	1.00	0.020	1.48	0.020	1.99
	RI-E	0.010	1.00	0.017	1.40	0.020	2.10
	RI-A	0.010	1.01	0.018	1.42	0.020	2.10
501	**RI-U**	0.010	1.00	0.016	1.43	0.031	1.21
	RI-E	0.010	1.00	0.015	1.50	0.020	2.10
	RI-A	0.010	1.01	0.015	1.49	0.018	2.21
501c	**RI-U**	0.012	0.90	0.015	1.44	0.028	1.67
	RI-E	0.010	1.00	0.015	1.51	0.021	1.88
	RI-A	0.012	0.91	0.015	1.50	0.024	1.99
1907	**RI-U**	0.010	1.00	0.016	1.42	0.020	2.21
	RI-E	0.010	1.00	0.015	1.50	0.020	2.13
	RI-A	0.010	1.01	0.015	1.48	0.019	2.11

Note that when the same study was carried out in 2-D (not shown here), the estimated optical properties were identical (variation of only $\sim$5%). As there are more degrees of freedom for the light propagation in 3-D as compared to 2-D (also 3-D model being more accurate compared to 2-D), the effect of reflection due to RI change might be more apparent in 3-D, thus leading to changes in the estimated optical properties. Moreover, the number of parameters to be estimated in IG-DOT is equal to be number of regions and any modeling error (here, the RI change) has to reflect in estimated region optical properties. Note that in only three out of six cases considered here (see Table I) resulted in more erroneous results for the reconstruction strategy of RI-U. In other three cases, the estimated optical properties were identical within 10%. The RI-A strategy resulted in erroneous results (not shown here), when the target RI values are not within $\sim$35% of the approximated values. The variations in RI for each region of breast reported in the literature is well within this range [10]–[13], [18].

The results obtained using three fiber layers data are given in Table II, with varying RI (given in the first column) for the RI-U strategy in the case of 1915 mesh. When compared to the estimated optical properties using single layer data (see

TABLE II
ESTIMATED OPTICAL PROPERTIES (IN mm^{-1}) OF EACH REGION OF 1915 MESH USING THREE FIBER LAYERS WITH RI-U STRATEGY FOR RI = 1.467, 1.4, AND 1.33

RI	*Adipose*		*Fibro-glandular*		*Tumor*	
	μ_a	μ_s'	μ_a	μ_s'	μ_a	μ_s'
RI = 1.467	0.010	0.99	0.016	1.44	0.033	1.17
RI = 1.4	0.010	1.01	0.015	1.51	0.025	1.89
RI = 1.33	0.009	1.05	0.014	1.58	0.013	19.4

The target values are given in the second row of Table 1.

Table I, third row), the errors have decreased by four times. But, they are still erroneous compared to RI-E and RI-A strategies (see Table I, fourth and fifth rows). Among the uniform RI values (1.467, 1.4, and 1.33; in RI-U strategy) for the meshes considered in this paper, RI value of 1.4 lead to lesser erroneous estimates of optical properties (also reflected in Table II). When results obtained using RI-U strategy with RI = 1.4 are compared against RI-E and RI-A strategies, the later strategies resulted in error reduction of at least 30%. Note that a similar trend was observed for other meshes (not shown here), indicating that the assumption of uniform RI in the IG optical imaging of breast leads to inaccurate estimation of optical properties.

The simulation studies with multiple tumors (specifically, breast having four regions with two of them being tumor region) were performed on the breast meshes. These results (not shown here) closely followed the observed trends of the case where breast had three regions (with only one tumor region).

Also, the estimated optical properties values did not change significantly (not more than $\sim$5%) when the λ in (3) was varied from 0.01 to 1000, which is expected in the case of LM minimization with J being close to positive definite (as NM $\gg$ NR) [8]. The effect of RI in traditional DOT is being explored currently, as it requires development of computationally efficient techniques in the estimation of optical properties along with the new methodology for the estimation of RI.

IV. CONCLUSION

In this letter, effect of RI in estimating optical properties in IG-DOT was studied using realistic patient 3-D breast meshes. It was shown that by assuming identical RI for different regions in breast could lead to erroneous estimation of optical properties. The *a priori* knowledge of RI should lead to accurate estimation of optical properties. More importantly, in cases where it is not feasible to obtain the RI of different regions of breast, using even approximate values of RI for each region of breast could lead to better estimates of optical properties in IG-DOT. Even though this study pertains to breast imaging, the trends and observations made in this study should hold good for other IG-DOT studies as well, including brain imaging. In conclusion, effective usage of image guidance by incorporating the RI variation (by approximation) in the computational model has improved the estimation of optical properties in IG-DOT.

ACKNOWLEDGMENT

The authors would like to thank Dr. S. Srinivasan, Prof. B. W. Pogue, and Dr. H. Dehghani for providing necessary 3-D meshes and NIRFAST package. They would also like to thank Mr. S. Gupta for providing useful inputs at the initial phase of this paper. R. P. K. Jagannath acknowledges university grants commission (UGC) junior research fellowship (JRF).

REFERENCES

[1] B. J. Tromberg, O. Coquoz, J. B. Fishkin, T. Pham, E. R. Anderson, J. Butler, M. Cahn, J. D. Gross, V. Venugopalan, and D. Pham, “Non-invasive measurements of breast tissue optical properties using frequency-domain photon migration,” *Philos. Trans. Roy. Soc. Lond. B*, vol. 352, pp. 661–668, 1997.

[2] A. P Gibson, J. C. Hebden, and S. R. Arridge, “Recent advances in diffuse optical imaging,” *Phys. Med. Biol.*, vol. 50, pp. R1–R43, 2005.

[3] B. J. Tromberg, B. W. Pogue, K. D. Paulsen, A. G. Yodh, D. A. Boas, and A. E. Cerussi, “Assessing the future of diffuse optical imaging technologies for breast cancer management,” *Med. Phys.*, vol. 35, pp. 2443–2451, 2008.

[4] S. R. Arridge, “Optical tomography in medical imaging,” *Inv. Probl.*, vol. 15, pp. R41–R93, 1999.

[5] B. Brooksby, B. W. Pogue, S. Jiang, H. Dehghani, S. Srinivasan, C. Kogel, T. D. Tosteson, J. Weaver, S. P. Poplack, and K. D. Paulsen, “Imaging breast adipose and fibro-glandular tissue molecular signatures using hybrid MRI-guided near-infrared spectral tomography,” *Proc. Nat. Acad. Sci. USA*, vol. 103, pp. 8828–8833, 2006.

[6] C. M. Carpenter, B. W. Pogue, S. Jiang, H. Dehghani, X. Wang, K. D. Paulsen, W. A. Wells, J. Forero, C. Kogel, J. B. Weaver, S. P. Poplack, and P. A. Kaufman, “Image-guided optical spectroscopy provides molecular-specific information in vivo: MRI-Guided spectroscopy of breast cancer hemoglobin, water and scatterer size,” *Opt. Lett.*, vol. 32, pp. 933–935, 2007.

[7] P. K. Yalavarthy, B. W. Pogue, H. Dehghani, C. M. Carpenter, S. Jiang, and K. D. Paulsen, “Structural information within regularization matrices improves near infrared diffuse optical tomography,” *Opt. Exp.*, vol. 15, pp. 8043–8058, 2007.

[8] P. K. Yalavarthy, B. W. Pogue, H. Dehghani, and K. D. Paulsen, “Weight-matrix structured regularization provides optimal generalized least-squares estimate in diffuse optical tomography,” *Med. Phys.*, vol. 34, pp. 2085–2098, 2007.

[9] C. M. Carpenter, S. Srinivasan, B. W. Pogue, and K. D. Paulsen, “Methodology development for three-dimensional MR-guided near infrared spectroscopy of breast tumors,” *Opt. Exp.*, vol. 16, pp. 17903–17914, 2008.

[10] F. P. Bolin, L. E. Preuss, R. C. Taylor, and R. J. Ference, “Refractive index of some mammalian tissues using a fiber optic cladding method,” *App. Opt.*, vol. 28, pp. 2297–2303, 1989.

[11] A. M. Zysk, E. J. Chaney, and S. A. Boppart, “Refractive index of carcinogen-induced rat mammary tumors,” *Phys. Med. Biol.*, vol. 51, pp. 2165–2177, 2006.

[12] H. Dehghani, B. Brooksby, K. Vishwanath, B. W. Pogue, and K. D. Paulsen, “The effects of internal refractive index variation in near-infrared optical tomography: A finite element modelling approach,” *Phys. Med. Biol.*, vol. 48, pp. 2713–2727, 2003.

[13] H. Dehghani, B. Brooksby, B. W. Pogue, and K. D. Paulsen, “Effects of refractive index on near-infrared tomography of the breast,” *App. Opt.*, vol. 44, pp. 1870–1887, 2005.

[14] T. Khan and A. Thoma, “Inverse problem in refractive index based optical tomography,” *Inv. Probl.*, vol. 22, pp. 1121–1137, 2006.

[15] M. Schweiger, S. R. Arridge, M. Hiroaka, and D. T. Delpy, “The finite element model for the propagation of light in scattering media: Boundary and source conditions,” *Med. Phys.*, vol. 22, pp. 1779–1792, 1995.

[16] H. Dehghani, B. Brooksby, K. Vishwanath, B. W. Pogue, and K. D. Paulsen, “Near infrared optical tomography using NIRFAST: Algorithms for numerical model and image reconstruction algorithms,” *Commun. Numer. Meth. Eng.*, vol. 25, pp. 711–732, 2009.

[17] B. Brooksby, S. Jiang, C. Kogel, M. Doyley, H. Dehghani, J. B. Weaver, S. P. Poplack, B. W. Pogue, and K. D. Paulsen, “Magnetic resonance guided near infrared tomography of the breast,” *Rev. Sci. Inst.*, vol. 75, pp. 5262–5270, 2004.

[18] X. Wang, “Estimation of effective scatterer size and number density in near-infrared tomography,” Ph.D. thesis, Dartmouth Coll., Hanover, NH, Feb. 2007.

[19] P. K. Yalavarthy, H. Dehghani, B. W. Pogue, and K. D. Paulsen, “Critical computational aspects of near infrared circular tomographic imaging: Analysis of measurement number, mesh resolution and reconstruction basis,” *Opt. Exp.*, vol. 14, pp. 6113–6127, 2006..